REPORT DOCUMENTATION PAGE

Form Approved
OMB No. 0704-0188

1. AGENCY USE ONLY *(Leave blank)*	2. REPORT DATE	3. REPORT TYPE AND DATES COVERED
	5.Jan.05	MAJOR REPORT

4. TITLE AND SUBTITLE
FREE TO ROLL INVESTIGATION OF UNCOMMANDED LATERAL MOTIONS FOR AN AIRCRAFT WITH VENTED STRAKES

5. FUNDING NUMBERS

6. AUTHOR(S)
CAPT BRYANT ELAINE M

7. PERFORMING ORGANIZATION NAME(S) AND ADDRESS(ES)
UNIVERSITY OF MARYLAND AT COLLEGE PARK

8. PERFORMING ORGANIZATION REPORT NUMBER
CI04-934

9. SPONSORING/MONITORING AGENCY NAME(S) AND ADDRESS(ES)
THE DEPARTMENT OF THE AIR FORCE
AFIT/CIA, BLDG 125
2950 P STREET
WPAFB OH 45433

10. SPONSORING/MONITORING AGENCY REPORT NUMBER

11. SUPPLEMENTARY NOTES

12a. DISTRIBUTION AVAILABILITY STATEMENT
Unlimited distribution
In Accordance With AFI 35-205/AFIT Sup 1

12b. DISTRIBUTION CODE

13. ABSTRACT *(Maximum 200 words)*

14. SUBJECT TERMS

15. NUMBER OF PAGES
8

16. PRICE CODE

17. SECURITY CLASSIFICATION OF REPORT	18. SECURITY CLASSIFICATION OF THIS PAGE	19. SECURITY CLASSIFICATION OF ABSTRACT	20. LIMITATION OF ABSTRACT

THE VIEWS EXPRESSED IN THIS ARTICLE ARE THOSE OF THE AUTHOR AND DO NOT REFLECT THE OFFICIAL POLICY OR POSITION OF THE UNITED STATES AIR FORCE, DEPARTMENT OF DEFENSE, OR THE U.S. GOVERNMENT.

AIAA 2005-236
43rd AIAA Aerospace Sciences Meeting and Exhibit
10-13 January 2005
Reno,NV

Free-to-Roll Investigation of Uncommanded Lateral Motions for an Aircraft with Vented Strakes

Elaine M. Bryant*
United States Air Force /University of Maryland, College Park, Maryland, 20742, USA

D. Bruce Owens†
NASA Langley Research Center, Hampton, Virginia, 23681, USA

and

Jewel B. Barlow‡
University of Maryland, College Park, Maryland, 20742, USA

A free-to-roll study of the low-speed lateral characteristics of the pre-production F/A-18E was conducted in the NASA Langley 12-Foot Low-Speed Tunnel. In developmental flight tests the F/A-18E unexpectedly experienced uncommanded lateral motions in the power approach configuration. The objective of this study was to determine the feasibility of using the free-to-roll technique for the detection of uncommanded lateral motions for the pre-production F/A-18E in the power approach configuration. The data revealed that this technique in conjunction with static data revealed insight into the cause of the lateral motions. The free-to-roll technique identified uncommanded lateral motions at the same angle-of-attack range as experienced in flight tests. The cause of the uncommanded lateral motions was unsteady asymmetric wing stall. The paper also shows that free-to-roll data or static force and moment data alone are not enough to accurately capture the potential for an aircraft to experience uncommanded lateral motion.

Nomenclature

CG		center of gravity
C_L	=	lift coefficient
C_l		total rolling moment coefficient
C_{lo}	=	rolling moment forcing function coefficient
C_{lp}		dynamic lateral stability coefficient, roll damping
$C_{l\beta}$	=	static lateral stability coefficient, spring effects
FTR		free-to-roll
HT	=	horizontal tail
LEF	=	leading edge flap
LEX	=	leading edge extension
PID	=	Parameter Identification
psf		pounds per square feet
TEF	=	trailing edge flap
TH		time history
VT	=	vertical tail
α		angle of attack
β	=	angle of sideslip
θ	=	pitch angle

* Graduate Student, Aerospace Engineering, College Park MD, Member AIAA.
† Aerospace Engineer, Flight Dynamics Branch, M/S 153, Associate Fellow, AIAA.
‡ Director Glenn L. Martin Wind Tunnel, Aerospace Engineering, College Park MD, Associate Fellow AIAA.

I. Introduction

IN 1996 the U.S. Navy's F/A-18E/F Super Hornet experienced uncommanded lateral motions, or wing drop, in the power approach (PA) configuration during developmental flight tests. These motions were not expected based on computational or experimental predictions during the design studies. Wing drop posed a potential risk to flight safety due to its occurrence at low altitudes and airspeeds. Based on data from investigative flight tests, wing drop was eliminated by retracting deployable vents located on the leading edge extension (LEX). The vents were located at the junction of the LEX and the wing. Figure 1 shows the location of the LEX and the LEX vent in the open position. Aligning the LEX vent flush with the wing and the LEX generates a LEX vents closed configuration. Although the LEX vents are not employed on the production version of the Super Hornet several efforts have been made to understand how opening the vents changed the flow topology that resulted in the uncommanded motions.

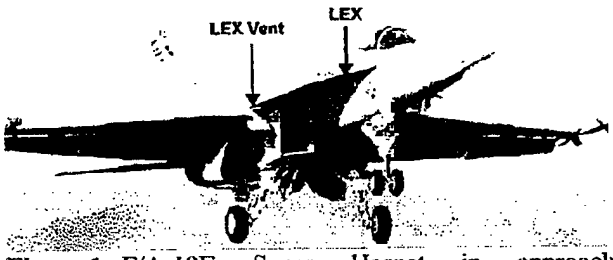

Figure 1. F/A-18E Super Hornet in approach configuration with the LEX vents open[5]

II. Motivation

Cook and Barlow[4-6] and Cook[3] report studies of the flow topologies on pre-production F/A-18E models that have shed much light on the characteristics of the flows. Some aspects of time dependence of forces and flows have been observed and reported but the models have always been held stationary. In actual flight events, the airplane motion responds in a transient manner to the changing forces as the flow changes. This experience provides a strong motivation for the application of the free-to-roll (FTR) method. This classical method offered promise for shedding additional light on the flight dynamics and aerodynamics of the lateral motions of the vented and unvented pre-production F/A-18E configurations. Owens et al[7] report on an extensive study of transonic uncommanded lateral motions of military aircraft using the free-to-roll technique, including the pre-production F/A-18E. The motivations, methods, and objectives for the application of the FTR method to the PA configuration parallel those for the transonic FTR tests of the pre-production F/A-18E. The physics of the aerodynamic phenomena associated with the uncommanded motions in the two cases are of course quite different.

III. Objective

The objective of this effort was to conduct a FTR feasibility test on the pre-production F/A-18E/F, to determine if this technique can be used to detect the uncommanded lateral motions as seen in flight. The goal was to compare indications of likelihood for uncommanded lateral motions from FTR method to the indications from the in-flight tests (Table 1) and the static data. Good correlation between the developmental flight-testing and the FTR testing, supported by static testing, would help establish capability for early identification of potential uncommanded lateral motions. In support of this goal a candidate FTR figure-of-merit (FOM) was proposed and assessments were carried out on: severity and types of model motions, unsteady aerodynamics, nonlinear aerodynamics and roll damping.

Aircraft, Flight and Maneuver	Angle of Attack (deg)	Angle of Sideslip (deg)	Leading Edge Flap Position (deg)	Trailing Edge Flap Position (deg)
F-1, 12, 19	15.0	0.0	30	40
F-2, 17, 07	12.1	-0.4	26	40
F-1, 26, 18	15.8	0.2	30	30
F-1, 26, 20	15.0	0.7	30	40
F-2, 39, 13	14.5	0.5	28	40
F-2, 39, 21	13.6	-2.5	15	30
F-2, 39, 23	13.8	1.2	15	40
F-2, 39, 24	13.7	0.0	15	40
F-2, 40, 41	13.3	-1.2	27	40
F-1, 06, 12	14.2	Not available	28	40

Table 1. Flight Test Results indicating α at which motion occured[5]

IV. Experimental Approach

The model used for both the static and the FTR testing was a 10% scale model of the pre-production F/A-18E. The model, constructed of balsa wood, plywood, fiberglass and aluminum, was outfitted with wing tip missiles, canopy, engine inlets, leading edge flaps (LEF), ailerons, flap shrouds, trailing edge flaps (TEF), vertical tail (VT), horizontal tail (HT) and LEX vents. The control surfaces were movable and could be set at specific values. For the data presented herein the HTs and rudders were at 0°. The LEX vents could be set to various open positions or it could be closed completely. Both tests were done in the NASA Langley 12-Foot Low-Speed Tunnel. The experiments were conducted at sea-level pressure and density with a freestream dynamic pressure of 4 psf resulting in a mean aerodynamic chord-based Reynolds number of $0.5X10^6$. Although numerous configurations were tested the paper will present LEX vents closed LEX vents open with the LEF = 10°, TEF = 30°, and ailerons = 30°. This positioning of the ailerons and TEF is referred to as the PA-half configuration. It is a slight modification from the PA configuration used in flight tests.

A. Static Testing

The static force and moments were measured using an internally mounted six-component strain gauge balance (NASA FF12). A series of both α- and β-sweeps were conducted with the configurations. Initially α-sweeps over the range $-4° \le \alpha \le 20°$ were conducted but for the majority of the runs a smaller α-range ($10° \le \alpha \le 20°$) with a higher resolution was chosen to cover the area of interest. Also, β-sweeps with a range of $-16° \le \beta \le 16°$ were performed in the smaller α-range to assess the static lateral characteristics. The data was sampled at a rate of 80 Hz for 10 seconds using a low-pass analog filter with cutoff frequency of 4 Hz. All data taken during the 10 second sample time was recorded. The paper will present both the time-averaged balance data as well as the time history of the balance signals over this 10 second window.

B. Free to Roll Testing

In the FTR test technique the model is constrained to roll about the longitudinal body axis. Switching from the static force and moment phase to the FTR requires replacing the balance with the FTR rig. Modifications to the interior of the model were required in order to accommodate the FTR rig. The FTR rig houses a resolver to measure the roll angle time history with an accuracy of 0.12 degrees. The roll angle signal was recorded at a rate of 200 Hz using a low-pass analog filter with a cutoff frequency of 4 Hz. Video of the lateral activity was also recorded. The FTR rig contains an air brake to stop the motion and allow the data point to start with a zero initial roll rate. The model's mass was balanced such that the lateral and vertical[JBB1] CG was located on the roll axis. The model's roll inertia was determined experimentally and found to be 0.40 slug-ft^2. This is less than 2 times the value required for dynamic scaling. Also, by knowing the roll inertia the total rolling moment, C_l, can be calculated by twice differentiating the roll angle time histories. The rolling moment time histories are then used in PID methods to determine C_{l_p}. The PID method used is described in reference 7. There were three ways to conduct a FTR test point: continuous pitch sweeps, pitch-pause and bank & release. For the continuous pitch-sweeps, the model was allowed to roll freely while going through a range of pitch angles. This type of test point quickly reveals any lateral activity over the α-range. The procedure for a pitch-pause point involved setting the model to the desired α and holding it there with the brake. Upon brake release the lateral motion was recorded. The information gathered reveals what the model will do when the roll angle and the roll rate are set to zero. The procedure for the bank & release points was to set the model at a certain roll angle and then the release the brake. The bank and release points are used to: assess how the model will reacted[JBB2] to a given initial rolling moment, assessment of roll-damping for the cases where no lateral activity existed at a pitch-pause point, and how inducing the rolling motion affected any motions observed previously. In order to quantify the lateral activity a FOM was used similar to the one used by Owens et al[7]. The FOM captures amplitude and rate effects. It is defined by: $p_{P-V} \equiv \left(\left| \frac{\Delta\phi}{\Delta t} \right| \frac{b}{2V_\infty} \right)_{\max}$. The plots of the FTR-FOM versus α were used to quantify the severity of the lateral activity.

The rolling motion can be described by a combination of forcing functions, roll damping, (C_{l_p}), and lateral stability (C_{l_β}) effects. Therefore, it is instructive when analyzing the data from a FTR test to consider the equation of motion in terms of the Euler angle ϕ as: $\frac{I_x \ddot{\phi}}{qSb} - C_{l_{\dot\phi}} \frac{\dot\phi b}{2V_\infty} - C_{l_\phi}\phi = C_{l_o}$ The foregoing equation is in the form of the classical mass-spring-damper system where: C_{l_o} represents an aerodynamic forcing function; C_{l_ϕ} represents the

spring constant which, along with the inertia, determines the frequency of oscillation; and C_{l_p} represents the damping coefficient. In the FTR technique, the use of C_{l_β} and C_{l_p} is kinematically equivalent. By measuring roll angle versus time, the FTR technique captures the composite effect of both static and dynamic forces acting on the model regardless of whether they are steady or unsteady.

V. Results and Analysis

This section will discuss the results for the vents-open and vents-closed configurations. The analysis will begin by using the FTR-FOM to show the severity and α-ranges of lateral activity for the configurations. Then detailed analysis will be presented for representative points within the α-range of lateral activity. The lateral activity of the two configurations is compared in Figure 2 using the FTR-FOM. The plot shows that for $12° \le \alpha \le 15°$ opening the

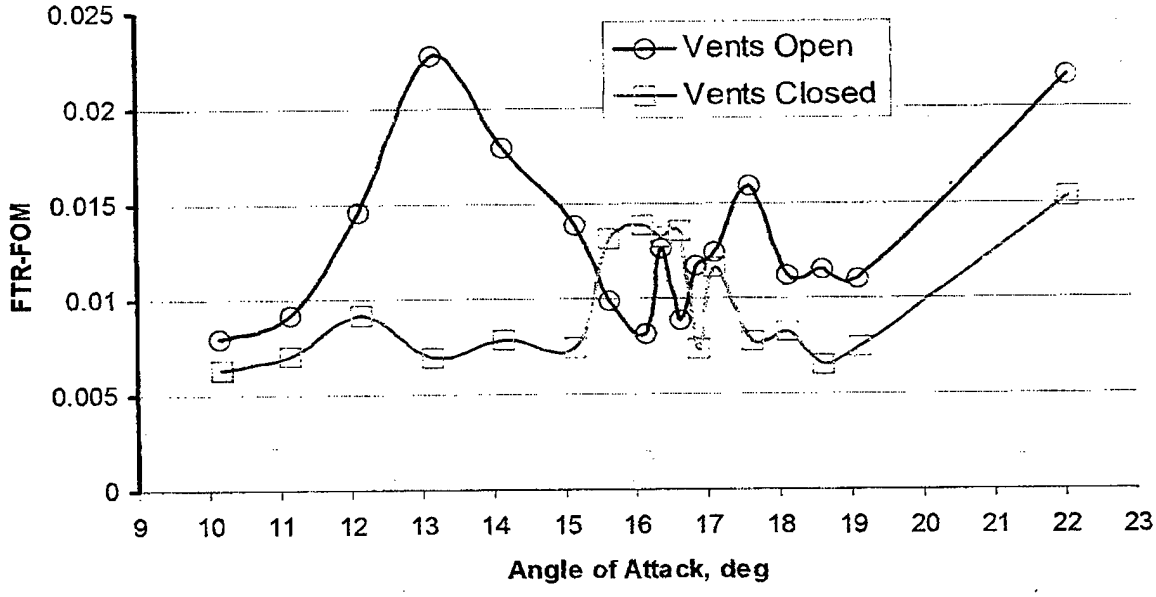

Figure 2. FTR-FOM Comparison between vents closed and vents open.

vents causes a significant increase in lateral activity with the maximum activity being at $\alpha = 13°$. This α-range directly correlates to the α-range in flight tests where wing drop occurred[5] (Table 1). For $\alpha = 15.5°$, 16°, and 16.5°, closing the vents increases lateral activity relative to the vents open position. For $\alpha = 16.25°$ and 17°, the severity of lateral activity is the same for both positions of the vents. For $\alpha = 16.75°$ and $\alpha \ge 17.5°$ opening the vents caused a significant increase in lateral activity. In summary, the FTR-FOM plot divides the α-range into three regions: $12° \le \alpha \le 15°$, $15.5° \le \alpha \le 17°$, and $\alpha > 17°$. For regions 1 and 3 there is a distinct reduction in lateral activity by closing the vents. In region 2 there is mixed results. Although not shown, repeatability of the FTR-FOM is excellent except at $\alpha = 17°$ and 19°. Since these points are above where activity was seen in flight the lack of repeatability has no impact on the following discussion.

The following discussion will use the FTR-FOM plot as the starting point for more detailed analysis. The points that will be analyzed will be one from region 1 and one from region 2 since this covers the α-range where wing drop was seen in flight. From region 1, $\alpha = 13°$ is chosen for analysis since this point shows the largest difference between vents open and close, and wing drop was first identified in flight at $\alpha = 13°$[5]. In order to show the amplitude and frequency change of the lateral activity between the two configurations, the roll angle time histories are shown for vents open and closed in Fig 3. The plot reiterates the large reduction in lateral activity by closing the vents. The cause of the rolling motion can be generated by any or all combinations of a forcing function, C_{l_0}, spring effects, C_{l_β}, and roll damping, C_{l_p}. Also, the aerodynamic terms may be unsteady. The following discussion will address each of these possibilities.

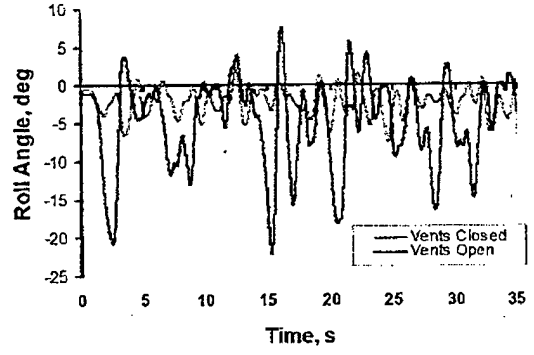

Figure 3. Roll Angle Time Histories for $\alpha = 13°$

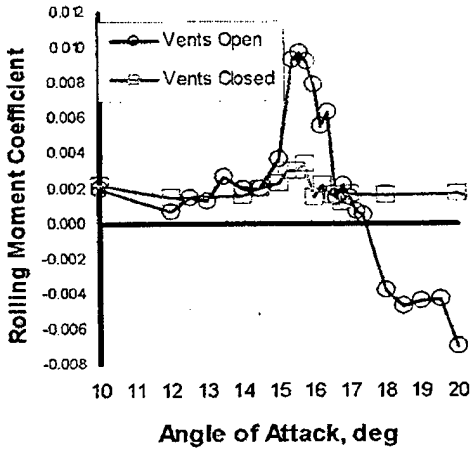

Figure 4. Comparison of vents open (run 44) to vents closed (run 10)

The steady state values of C_{lo} are shown in Fig. 4 with a plot of rolling moment coefficient with respect to α. (Note. There is a $C_l = 0.002$ offset for both configurations below $\alpha = 17°$. The cause of this asymmetry in the data is probably due to tunnel sidewash and/or model asymmetrics. The data will be discussed relative to the offset.) The data shows that no time-averaged value of C_{lo} exists at $\alpha = 13°$ to cause the significant lateral activity for the vents-open configuration. Balance rolling moment time history signals indicate that C_{lo} is unsteady. Figure 5 compares the balance rolling moment time history of the vents open to vents closed at $\alpha = 12°$. No balance data was taken for the vents closed case at $\alpha = 13°$ so a comparison is made at $\alpha = 12°$. The characteristics of the balance signals at $\alpha = 12°$ is indicative of the balance signals where data was taken in the $12° \leq \alpha \leq 15°$ for the two configurations. The plot clearly shows that the vents-open configuration has aperiodic rolling moment spikes with sufficient amplitude and low enough frequency to cause rigid body rolling motion. Figure 6 shows the static lateral stability characteristics, $C_{l\beta}$, for the vents-open configuration. The plot shows that the model has a strong spring, $C_{l\beta}$, which contributes to the lateral activity seen in the roll angle time history plot of Fig. 3. The lift characteristics of the two configurations are shown in Fig. 7. The data shows that the vents-open configuration produces a more non-linear lift curve than the vents-closed configuration. Nonetheless, there are no sharp breaks with significant loss in lift. This data shows that even though no time-averaged rolling moment spike occurs (Fig. 4) or no significant changes in the time-averaged lift curve slope (Fig. 7) that the wing can be experiencing an unsteady aerodynamic forcing function that causes uncommanded lateral motions. It is then left to the FTR technique to show that this unsteady aerodynamic forcing function produces undesirable lateral activity. The roll damping characteristics are shown in Fig. 8. The plot shows no significant difference or change in roll damping characteristics over the α-range where activity was seen in flight. Therefore, roll damping is not a cause of the lateral activity. Therefore, the lateral activity produced by opening the vents in the $12 \leq \alpha \leq 15°$ is caused by a strong spring and an unsteady forcing function.

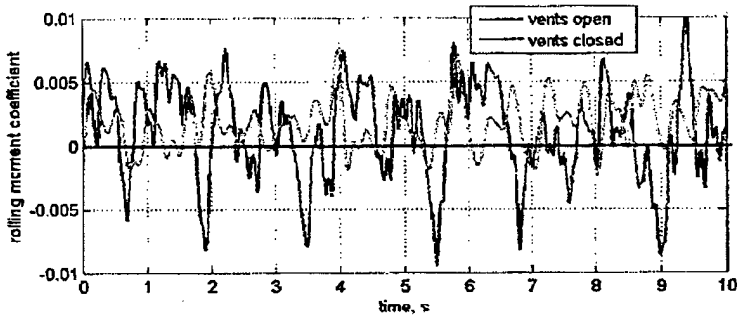

Figure 5. Balance rolling moment signal time history for vents open (run 44 pt2) and vents closed (run 10 pt 8), α 12°.

From region 2, the lateral activity at $\alpha = 16°$ will be analyzed since this occurs at a critical state as indicated in the static rolling moment curve of Fig. 4 and is the point in region 2 where the lateral activity between the two configurations is a maximum as indicated by the FTR-FOM plot of Fig. 2. The roll angle time histories of the vents-closed and -open positions are shown in Fig. 9. Prior to the FTR testing it was expected that the vents-open position would exhibit significant wing drop at α's around 16° because the wing is going through stall and there is a

Figure 8. Roll Damping Effects, $\alpha = 13°$

Time, s

Figure 9. Roll Angle Time Histories for $\alpha = 16°$, pt 99,pt 116.

significant spike in the rolling moment curve (Fig. 4). The wing stall (Fig. 7) and rolling moment characteristics (Fig. 4) are benign for the vents-closed configuration. Therefore, it was expected that the vents-closed configuration would not exhibit significant lateral activity. Fig. 9 shows with a plot of the roll angle time histories that just the opposite happened. Compared to vents-open activity at $\alpha = 13°$, the vents-closed activity at $\alpha = 16°$ is of smaller amplitude and frequency. This is reflected in the FTR-FOM plot, Fig.2. The cause of the lateral motion characteristics for the two configurations at $\alpha = 16°$ will now be explained using static and dynamic data.

The time-averaged value of C_{lo} shown in Fig. 4 shows that at $\alpha = 16°$ there is a significant value of C_{lo} (0.006) for the vents-open case. The TH plot for the vents-open configuration shows a left wing down trim point which contradicts the rolling moment data of Fig 4. Previous data[5] from test 123 shows that this same 10% F/A-18E model can exhibit negative rolling moment spikes. Evidently, when the model was changed from the static force & moment mount to the FTR the model had a tendency to stall such that a left wing down rolling moment was generated as in test

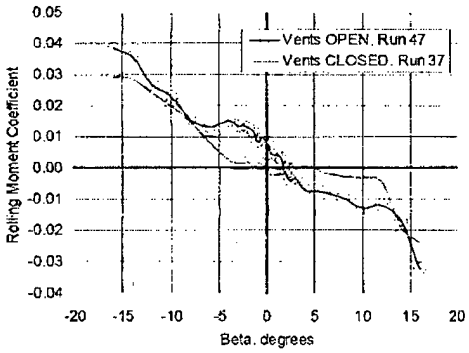

Figure 10. Rolling Moment